Journal of Zhejiang University-SCIENCE A (Applied Physics & Engineering)
ISSN 1673-565X (Print); ISSN 1862-1775 (Online)
www.zju.edu.cn/jzus; www.springerlink.com
E-mail: jzus@zju.edu.cn

Numerical investigation on the drag reduction properties of a suction controlled high-rise building*

Chao-rong ZHENG†, Yao-chun ZHANG

(*School of Civil Engineering, Harbin Institute of Technology, Harbin 150090, China*)

†E-mail: flyfluid@163.com

Received Oct. 2, 2009; Revision accepted Apr. 12, 2010; Crosschecked June 9, 2010

Abstract: To reduce the wind-induced drag and improve the wind-resistance performance of a high-rise building, steady suction control is introduced into the building structure. Based on validation of the numerical methods by experiment with suction control over the flow separation of a 3D backward-facing step, the Reynolds stress equation model is used to investigate the drag reduction (DR) properties of a high-rise building whose side faces are controlled by all-height suction. Effects of the orifice geometrical parameters and suction flux parameters on the DR and the separation control are analyzed, and the detailed flow fields are shown to clarify the mechanism of suction control. The results indicate that suction control is very effective in reducing the wind loads on the high-rise building model, and only the dimensionless suction flux dominates. Lastly, the power consumed and the counterforce induced by suction are discussed, the suction models become the "zero-drag" model under certain suction angles.

Key words: High-rise building, Numerical simulation, Suction control, Drag reduction (DR), Power, Mechanism analysis
doi:10.1631/jzus.A0900593 **Document code:** A **CLC number:** TU973.213; V211.3

1 Introduction

As a result of the extensive utility of high-strength and light-weight materials in construction, civil engineering structures, such as high-rise buildings and large-span structures, tend to be more flexible and have a lower damping ratio. Therefore, they are very sensitive to wind excitation, and the wind-resistance design has gradually become the dominant factor in structural designs (Kareem *et al*., 1999; Kijewski-Correa *et al*., 2006; Luo and Han, 2009). Wind-resistance design for high-rise buildings, such as the strength, displacement and habitational comfort, are confronted with severe challenges under strong wind conditions, and the claddings frequently suffer from destruction, creating substantial costs. Consequently, it is very important and necessary to investigate the physical mechanism of wind loads on high-rise buildings, and to take aerodynamic measures to reduce the wind loads and wind-induced responses.

Apparently, the most effective way to reduce wind-induced responses is to eliminate the excitation source, and knowledge of the aerodynamic measures for drag reduction can dramatically improve the wind-resistance performance of these structures. According to Fox *et al*. (2008), the pressure drag, which was mainly generated by the flow separation in the boundary layer, occupied more than 90% of the wind-induced drag on the bluff bodies. Flow separation can lead to complex flow fields around high-rise buildings, and can bring extreme suction forces on the corners of the side face and top face, together with significant suction forces on the leeward face, downstream the side face and the top face (Simiu and Scanlan, 1996). Consequently, it is necessary to adopt flow control techniques to restrain or avoid the separation, and among these techniques, the suction control method has already been widely used in the domains of aerospace (Greenblatt and Wygnanski, 2000;

* Project (No. 59895410) supported by the National Natural Science Foundation of China

Huang *et al*., 2004; 2007), pipeline transportation (Uruba *et al*., 2007), and fluid machinery (Song *et al*., 2005).

The suction method is an active means to control the overall flowfield around the bluff or streamlined body, though it requires power to drive the suction mechanism. The basic principle of suction control is to remove the low-velocity fluid from the boundary layer and to deflect the high-momentum free-stream fluid towards surfaces of the body (Greenblatt and Wygnanski, 2000; Schlichting and Gersten, 2000), with the aim of restraining or avoiding separation, thereby increasing the lift force and decreasing the drag force.

To reduce the wind-induced drag and improve the wind-resistance performance of high-rise buildings, the steady suction control is introduced into the building structures, and the performance of wind-load reduction for an all-height suction high-rise building is numerically investigated through the Reynolds stress equation model (RSM). Effects of the orifice geometrical parameters and the suction flux parameters on the drag reduction (DR) property are analyzed, and detailed flow fields (including the Reynolds-averaged stream and vorticity fields) are shown to clarify the mechanism of suction control. Moreover, the power consumed and the counterforce induced by suction are discussed. The overall aim of this paper is to provide the preliminary reference information for practical application of the all-height suction to high-rise buildings.

2 Numerical methods

The analytical model, with a height of 600 mm (H=600 mm) and a width (depth) of 162 mm (B=D=162 mm), was a high-rise building baseline model which had been investigated through wind tunnel tests (WTT) by Zhang *et al*. (2004). In the WTT, the high-rise building model had a length scale of 1/S=1/300, and the mean velocity at the top of the model was set to V_H=13.5 m/s (which was also defined as the referenced velocity V_∞ in this study). Thus, the Reynolds number based on width of the model and the V_H was about 1.51×10^5. Only the models with one face normal to the wind direction and the all-height suction models with a change of suction in the horizontal plane were studied in this research.

Fig. 1 shows a sketch of suction control on an arbitrary cross-section of the model, where the slot size d denotes the width of the slot and g denotes the distance from the left-side of the suction slot to the front corner of the side face. According to the previous study on comparison of the DR property for the suction models with six slot schemes on the side face (g=0, g=3%D, g=5%D, g=8%D, g=10%D and the suction slot locates at the rear of the side face, respectively) (Zheng, 2010), the optimal slot position on the side face was g=3%D, so the value of g=3%D was adopted for all the models in this study. The suction angle θ denotes the direction of air suction, and is defined as 0° when the suction direction is identical to the wind direction. θ reflects the relationship between the component velocity normal to the side face V_c and the along-wind suction velocity component V_{ca} (V_{ca}=$V_c$cot θ).

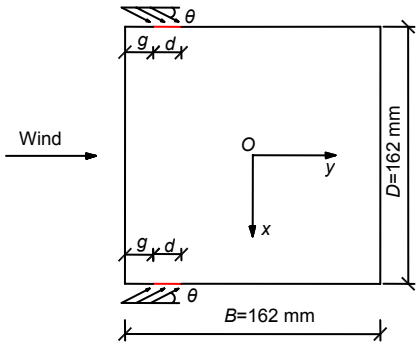

Fig. 1 Sketch of suction control on an arbitrary cross-section of the model

The computational domain, with a length of 6 m, a width of 3 m and a height of 2 m, was discretized by the multi-block structured and non-uniform orthogonal grid. Before the parameter analysis, four near-wall grid resolutions were initially compared to check the grid independence, which will be discussed in the following sections.

The Reynolds-averaged Navier-Stokes (RANS) equations were adopted to match the grid resolution, and discretizations of the incompressible governing equations were accomplished by the Computational Fluid Dynamics (CFD) code FLUENT 6.2, using the finite-volume method.

The turbulence model of RSM was used to close the RANS equations, and the non-equilibrium wall

function was introduced to simulate the low-Reynolds flow near the wall. The second-order upwind and the second-order central differencing scheme were adopted to discretize the convective terms and the diffusive terms in the N-S equations, respectively. Moreover, the pressure-velocity decoupling of the discretized equations was implemented by the semi-implicit method for pressure-linked equations (SIMPLE) algorithm, which is suitable for steady calculations.

The inflow boundary condition was programmed by the user defined function (UDF) in FLUENT. The inflow velocity profile was set as the power law $V(z)=V_{10}(Sz/10)^{0.22}$ (the mean velocity at the height of 10 m was set to V_{10}=7.148 m/s) to simulate the terrain roughness of C type in Chinese Load Code (GB50009-2001, 2002), where z is the height away from the ground. The turbulence kinetic energy and turbulence dissipation rate were expressed by the empirical formulae (Tu *et al*., 2008; Zheng and Zhang, 2008):

$$k(z)=1.5[I(z)\times V(z)]^2, \tag{1}$$

$$\varepsilon(z)=0.09^{3/4}k(z)^{3/2}/l, \tag{2}$$

where the turbulence intensity $I(z)$ was adopted from the third type of the terrain roughness (corresponding to the terrain roughness of C type in GB50009-2001) in the Australian/New Zealand Standard, expressed as

$$\begin{cases} I(z)=0.271,\ Sz \le 5\ \text{m}, \\ I(z)=-0.0357\ln(Sz)+0.3255,\ Sz>5\ \text{m}, \end{cases} \tag{3}$$

and the turbulence length l was set as $0.07H$.

The outflow boundary condition was set as the fully developed turbulence in the outlet. For the suction slots, the boundary was set as the velocity-inlet boundary condition under suction, and it was changed to the no-slip wall boundary when there was no suction. As for the other surfaces of the computational domain and the analytical model, the no-slip wall boundary condition was used to simulate the wall boundary in the wind tunnel test.

Applicability of the numerical methods stated above were verified by an experiment conducted by Uruba *et al*. (2007) with suction control over the flow separation of a 3D backward-facing step (Zheng, 2010), and the results indicated that the dimensionless reattachment length x_r/h (h denotes the step height) from the numerical simulation and experiment showed good agreement for the tested suction flow coefficient with a maximum error of 10%, and thus validating the numerical methods.

3 Definitions for main parameters

The quantity of the DR is characterized by the coefficients of pressure reduction for test points (C_{PRi}) and for surfaces (C_{PR}) of the suction model, which are defined as

$$C_{PRi}=1-C_{PCi}/C_{PBi}, \tag{4}$$

$$C_{PR}=1-C_{PC}/C_{PB}, \tag{5}$$

where C_{PCi} and C_{PBi} is the mean pressure coefficient for point of the model with and without suction, respectively, and C_{PC} and C_{PB} is the area-weighted-averaged mean pressure coefficient for surface of the model with and without suction, respectively. Accordingly, the coefficients of drag reduction (C_{DR}) and along-wind base moment reduction (C_{MR}) are defined to denote reduction for the drag and the along-wind base moment of the suction model, respectively. When $0<C_{DR}$ (or C_{MR})≤ 1.0, it means that suction can reduce the drag or the base moment of the baseline model, and C_{DR} (or C_{MR})>1.0 means that the suction has changed the direction of the drag force or the base moment.

The dimensionless suction flux C_Q is defined as the ratio of air mass flux through one of the slots over the referenced mass flux:

$$C_Q=\rho_c Q_c/(\rho_e Q_\infty)=\rho_c dV_c H/(\rho_e DV_\infty H), \tag{6}$$

where the density of the suction air and the incoming flow are both set to $\rho_c=\rho_e=1.225$ kg/m^3, and Q_c and Q_∞ are the volumes flux through one of the slots and the referenced flux. C_Q is defined as negative for suction.

4 Grid independence checking

Fig. 2 shows the near-wall grid configuration around planes z/H=2/3 of the baseline models or the

suction models, and the grid near the slots are locally refined (there are 5, 8 and 12 grid cells to discretize the slot with d=3, 5 and 8 mm, respectively). The overall number of grid cells for different cases involved in this study was about 1.08–1.20 million. The grid quality around planes z/H=2/3 of the baseline models with different near-wall grid resolutions (the minimum near-wall grid size normal to the model was 2 mm (D/81), 3 mm (D/54), 5 mm (nearly D/32) and 9 mm (D/18), respectively) are shown in Fig. 3, where x' and the numbers 0–4 are used to determine locations of the mesh centers around planes z/H=2/3. The grid quality was expressed by the wall unit $y^+=\Delta y u_\tau/\nu$, where half of the least grid size normal to surfaces of the baseline models were Δy=1.0, 1.5, 2.5 and 4.5 mm, respectively. $u_\tau=(\tau_w/\rho_e)^{0.5}$ is the frictional velocity, where τ_w is the near-wall shear stress, and ν is the kinematic viscosity.

As shown in Fig. 3, y^+ for the baseline model with Δy=2.5 mm are mainly located between 30 and 300, which is under consideration by the wall function formulation.

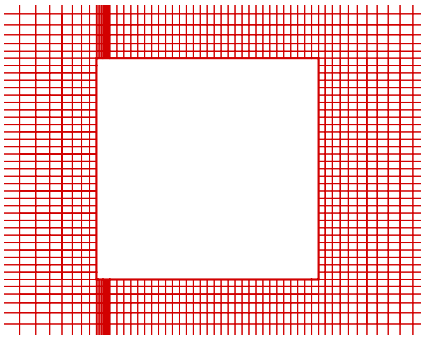

Fig. 2 Near-wall grid configuration around plane z/H=2/3 of the baseline model or suction models

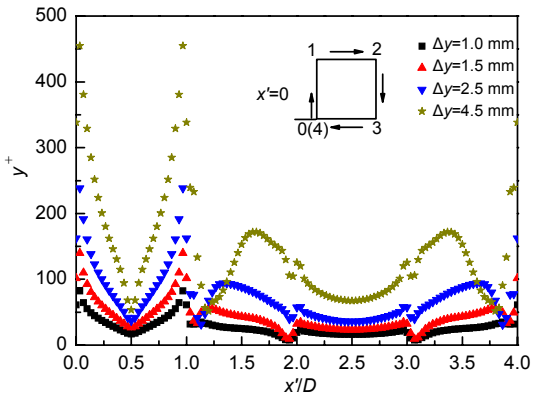

Fig. 3 Near-wall grid quality y^+ around planes z/H=2/3 of the baseline models with different grid resolutions

Comparison of C_{PBi} around planes z/H=2/3 of the baseline models is shown in Fig. 4, C_{PBi} is close to each other except for the grid scheme with Δy=4.5 mm. So the baseline model with Δy=2.5 mm is suitable for the computation.

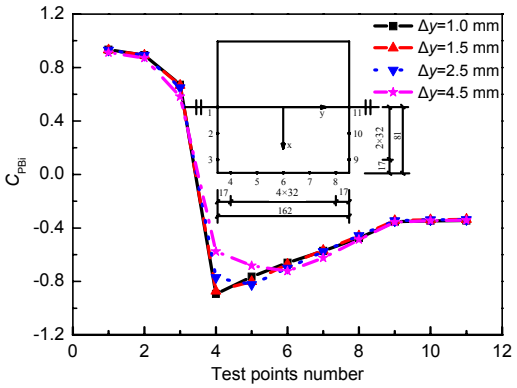

Fig. 4 Effect of near-wall grid size on C_{PBi} of the test points on the plane z/H=2/3

Comparison of C_{PCi} around planes z/H=2/3 of the suction models (C_Q=−0.0457, θ=15° and d=5 mm) is shown in Fig. 5, C_{PCi} for the test points are close to each other except for point 4, so the suction model with Δy=2.5 mm is also suitable for the computation. Furthermore, convergence of numerical computation for the suction models with less near-wall grid size is worse than that for the suction model with Δy= 2.5 mm, because the stretch ratio of the grid for the former models are larger than the latter model when using the same overall number of grid cells. Under the circumstance, the suction models with Δy=2.5 mm are analyzed in this study.

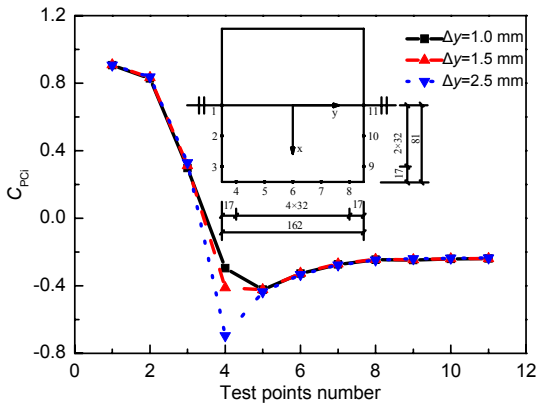

Fig. 5 Effect of near-wall grid size on C_{PCi} of the test points on the plane z/H=2/3

5 Results and discussions

Effects of θ and d on the along-wind C_{DR} and C_{MR} of the suction models under C_Q=−0.0457 are shown in Fig. 6. Though C_{DR} and C_{MR} are slightly decreased with increasing increments of θ or d, the maximum variation between all the models is less than 15%. Therefore, θ or d shows little influence on the DR of the suction models under the same C_Q.

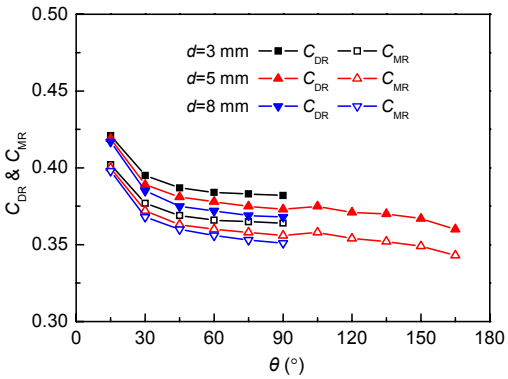

Fig. 6 Effects of the suction angle and the slot size on C_{DR} and C_{MR}

Moreover, the Reynolds-averaged pressure and stream fields around planes z=2H/3 of the suction models under the extreme suction angles (θ=15°, 90° and 165°) are compared in Fig. 7 for the suction models under C_Q=−0.0457 and d=5 mm, and Fig. 8 shows the vorticity fields around planes z=2H/3 of these models with a spacing of 100 per second, where the value is larger for the contours inside. The results indicate that θ or V_{ca} shows little influence on the DR of the suction models under the same C_Q.

Put simply, the suction works as a sink: only its capacity (C_Q) is important for the DR, while the orifice geometrical parameters (such as θ and d) and the suction velocities (such as V_c and V_{ca}) show little influence on the DR.

The effect of C_Q on C_{PR} for the surfaces, along-wind C_{DR} and C_{MR} of the suction models is shown in Fig. 9, and the models involved in the following section have a suction angle θ of 15° and a slot size d of 5 mm. With increasing increments of the absolute value of C_Q, the values of C_{PR}, C_{DR} and C_{MR} increase rapidly (with the odd exception of C_{PR} for the side face when the absolute value of C_Q is less than 0.0229), and the DR for the windward face, the along-wind drag and the along-wind base moment are more significant than that for the leeward face and the top face. However, too large absolute value of C_Q will be restrained in the practical application, due to the consideration of the energy requirement, discomfort for the environment and the suction-induced noise.

As C_{PR} for the side face or the top face is mainly determined by the flow separation and reattachment, and C_{PR} for the leeward face is mainly related to the curvature and width of the wake, removal of the separation by suction can significantly influence the property of DR for these faces.

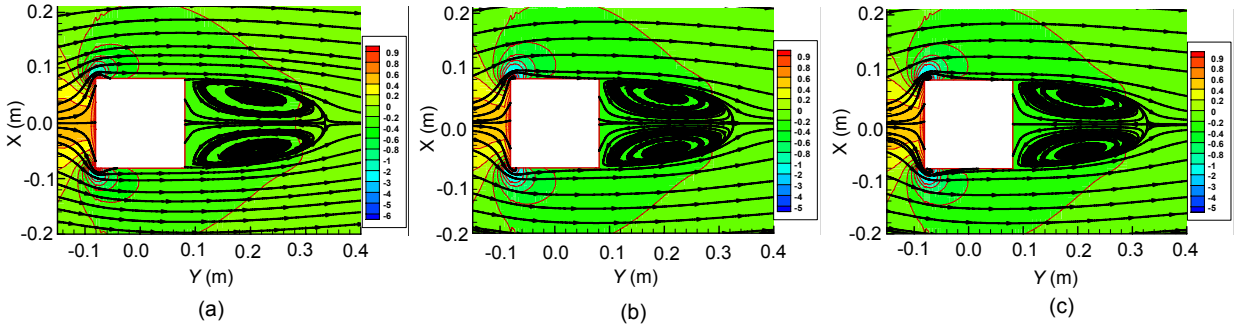

Fig. 7 Comparison of the Reynolds-averaged stream and pressure fields around the suction models

(a) θ=15°; (b) θ=90°; (c) θ=165°

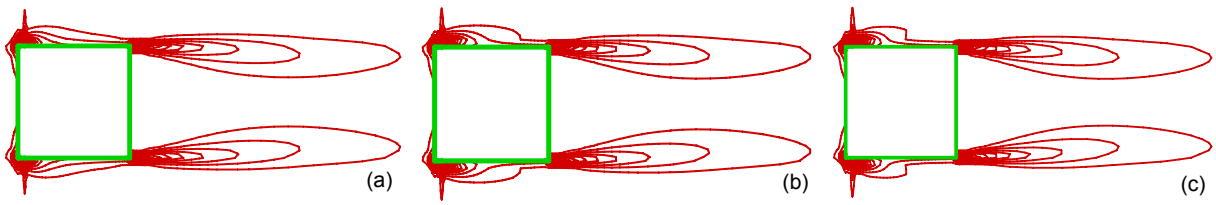

Fig. 8 Comparison of the Reynolds-averaged vorticity magnitude around the suction models

(a) θ=15°; (b) θ=90°; (c) θ=165°

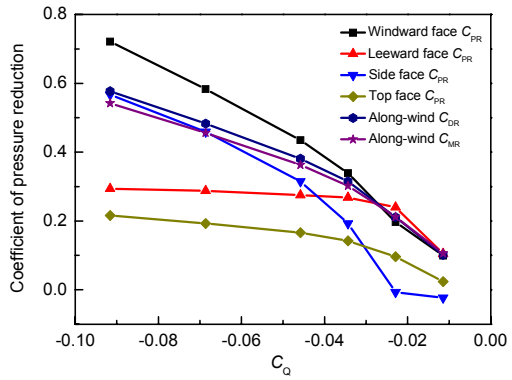

Fig. 9 Effect of the dimensionless suction flux C_Q on C_{PR}, C_{DR} and C_{MR}

On one hand, separation flows downstream along the side face are controlled by suction, so the suction forces are decreased. On the other hand, the flows near the slots are accelerated in the counter-wind direction by suction, and the small scale vortices appear near the slots, so the suction forces are greatly increased in these regions. To sum up, two kinds of effects determine C_P on the side face, and the effect of the small scale vortices will be dominating under less negative C_Q. These statements explain why there is no improvement of C_P on the side face when the absolute value of C_Q is less than 0.0229.

To depict effect of C_Q on the space distribution of C_{PRi} for the suction models, Fig. 10 shows contours of C_{PRi} on surfaces of the suction models under C_Q=−0.0229, −0.0457 and −0.0686, respectively. The big arrowheads in the figures denote the direction of the exterior flow, and the small arrowheads denote the direction of the air suction.

C_{PRi} are almost positive for the entire surfaces of the suction models except for the front corners of the side face and top face (Fig. 10), so it can be concluded that suction is very effective on the DR for the high-rise building. C_{PRi} on two sides of the windward face, front corners of the side face and top face are notably changed, denoting the intensive control of the flows on these zones; however, it is relatively uniform on the leeward face.

Moreover, the distribution regularity of C_{PRi} on the surfaces is almost the same for the suction models with different C_Q, though C_{PRi} is larger under larger absolute value of C_Q, and changes of C_{PRi} on the leeward face and top face are less than that on the windward face and side face as C_Q is changed.

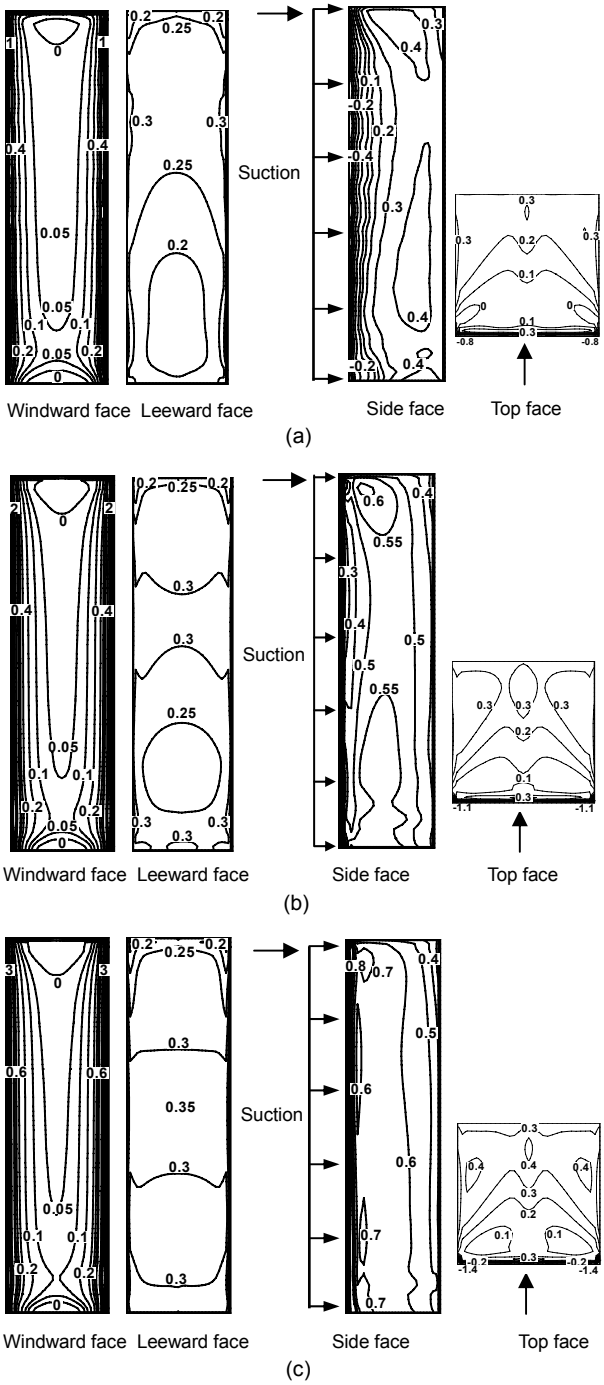

Fig. 10 Contours of C_{PRi} on surfaces of the suction models with different C_Q

(a) C_Q=−0.0229; (b) C_Q=−0.0457; (c) C_Q=−0.0686

To analyze the mechanism of suction control on the DR for the high-rise building model, the Reynolds-averaged streamlines around planes z/H=2/3 of the models with and without suction are compared in Fig. 11, and Fig. 12 shows contours of the vorticity magnitude around planes z/H=2/3 of these models.

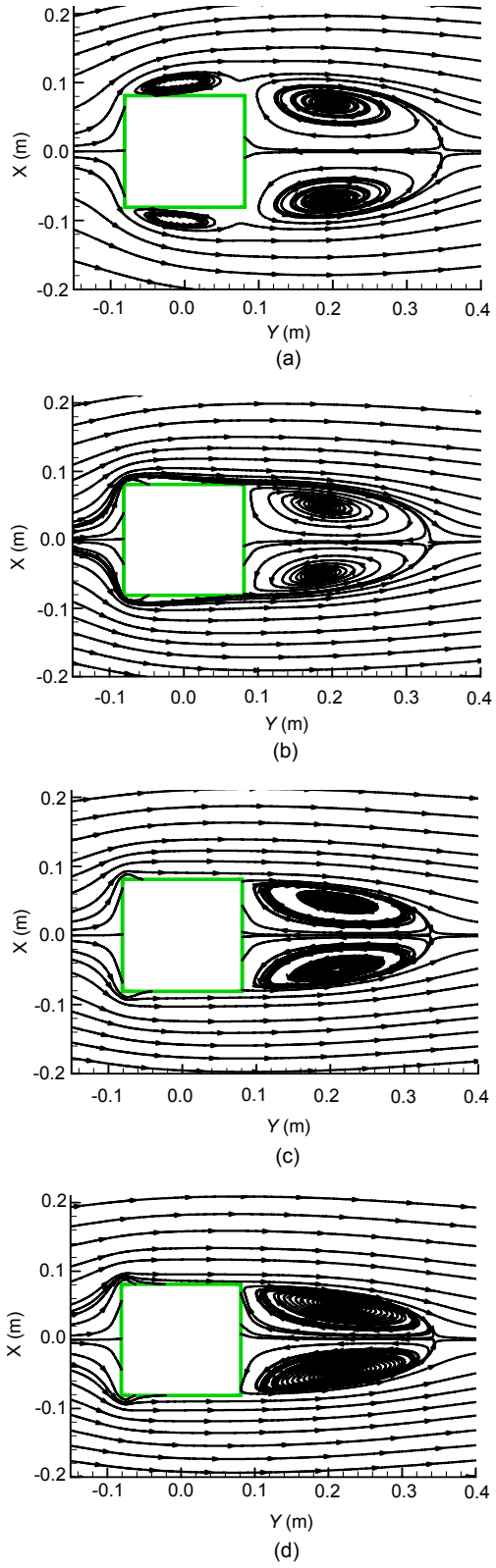

Fig. 11 Comparison of the Reynolds-averaged streamlines around planes z/H=2/3 of the models with or without suction
(a) C_Q=0; (b) C_Q=−0.0229; (c) C_Q=−0.0457; (d) C_Q=−0.0686

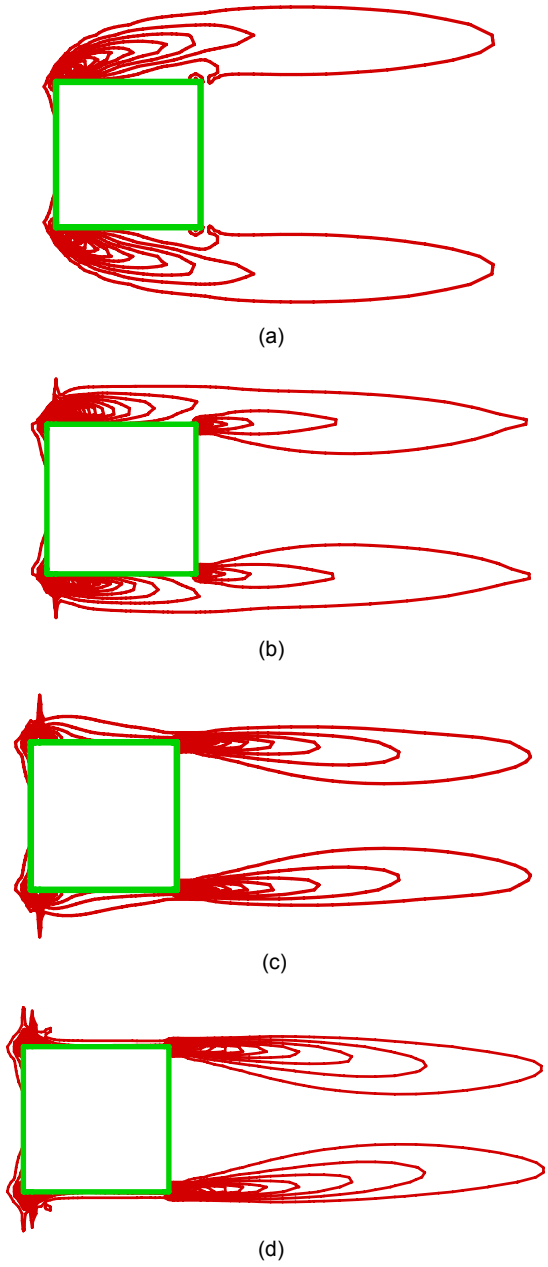

Fig. 12 Contours of the vorticity magnitude around planes z/H=2/3 of the models with and without suction
(a) C_Q=0; (b) C_Q=−0.0229; (c) C_Q=−0.0457; (d) C_Q=−0.0686

As shown in Fig. 11a, the region around the baseline model exhibits several flow phenomena, such as separation and recirculation. There are significant large scale vortices near the side face, with little reattachment occurring, so the curvature and width of the wake are very large. A wide region with large vorticity magnitude appears near side faces of the baseline model in Fig. 12a; however, the near-wall

vorticity magnitude downstream the side face is very small.

From Figs. 11b–11d and Figs. 12b–12d, it can be seen that suction can bring more flow around the windward face (as the vorticity magnitude is greatly increased on corners of the windward face), restrain the flow separation and development of the vortices, and make the streamlines deflect to the side face, so that the large scale vortices near the side faces disappear. As well, much more flow reattachment can be observed and the vorticity magnitude away from the side face is notably reduced. The reattachment flows re-separate at the trailing edge of the side face, which results in a narrow wake with high vorticity magnitude behind the leeward face. However, the regions near the slots have two visible cavities, which mean that there are small scale vortices in these regions (the phenomenon is not very evident because of the relative coarse grid near the side face), so the suction forces are greatly increased. Therefore, attention should be paid to the aerodynamic modifications for corners of the slots to restrain the development of the vortices.

With increasing increments of the absolute value of C_Q, more flow around the windward face is generated, while the flows re-separate at the trailing edge of the side face, which results in less curvature of the recirculation, a narrower wake and a higher vorticity magnitude for the wake. So the all-height suction model with larger C_Q will have more significant DR.

Simiu and Scanlan (1996) pointed out that when the flowfield around the bluff body without suction had a larger curvature of the recirculation and wider wake, the wind-induced drag would be larger. So for the mechanism of suction control on the DR for the high-rise building, it can be concluded that suction can bring more flow around the windward face, restrain the flow separation and decrease curvature of the recirculation and width of the wake.

Effect of suction on the length of the wake can be discussed in two aspects. First, suction can reduce the curvature of the recirculation and the width of the wake, so the length of the wake will increase; second, suction will remove part of the along-wind momentum from the separation flows, so the distance of its movement in the wake will decrease. These statements explain why the length of the wake for the suction models are close to the baseline model around the planes z/H=2/3.

Furthermore, the Reynolds-averaged streamlines around planes x=0 of the models with and without suction are compared in Fig. 13. The circulation zone and size of the large scale vortex behind the leeward face is notably reduced with increasing increments of the absolute value of C_Q.

In addition, the separation flow restrained by suction control is accompanied with a reduction of the boundary layer thickness near the side face. According to Newton's law of viscosity, reducing the boundary layer thickness can lead to an increase of the shear stress near the side faces, which is accompanied by the increase of the near-wall vorticity magnitude and the friction drag (though it is small compared to the pressure drag). The phenomena are confirmed by the contours of the vorticity magnitude in Fig. 12, where the high vorticity magnitude region near the side face is reduced by suction, and the vorticity magnitude along the side face is increased.

For a high-rise building with its side faces controlled by all-height suction, the power input for suction can be calculated by the following formula derived from the kinetic energy theorem (Zheng, 2010)

$$P=2\times\rho_c Q_c V^2/2=\rho_c dHV_c(V_c^2+V_{ca}^2), \tag{7}$$

where V is the compositional velocity superposed by V_c and V_{ca}. Based on Eqs. (6) and (7), as DR for the all-height suction model is mainly determined by C_Q, and P is proportional to cubic of V_c, the suction models with large ρ_c and d together with θ=90° are preferred under the same C_Q.

Furthermore, the counterforce is caused by the air suction, and the component force against the wind direction can be derived from the momentum theorem (Zheng, 2010):

$$F_y=2\rho_c dHV_c V\cos\theta=2\rho_c dHV_c V_{ca}, \tag{8}$$

and the equivalent against-wind drag coefficient and base moment can be calculated:

$$C_D'=F_y/(\rho_c V_\infty^2 DH/2), \tag{9}$$

$$M_x'=F_y\times H/2. \tag{10}$$

Thus, C_D' or M_x' is another way to compute DR, and suction models with larger d and less θ can bring more DR.

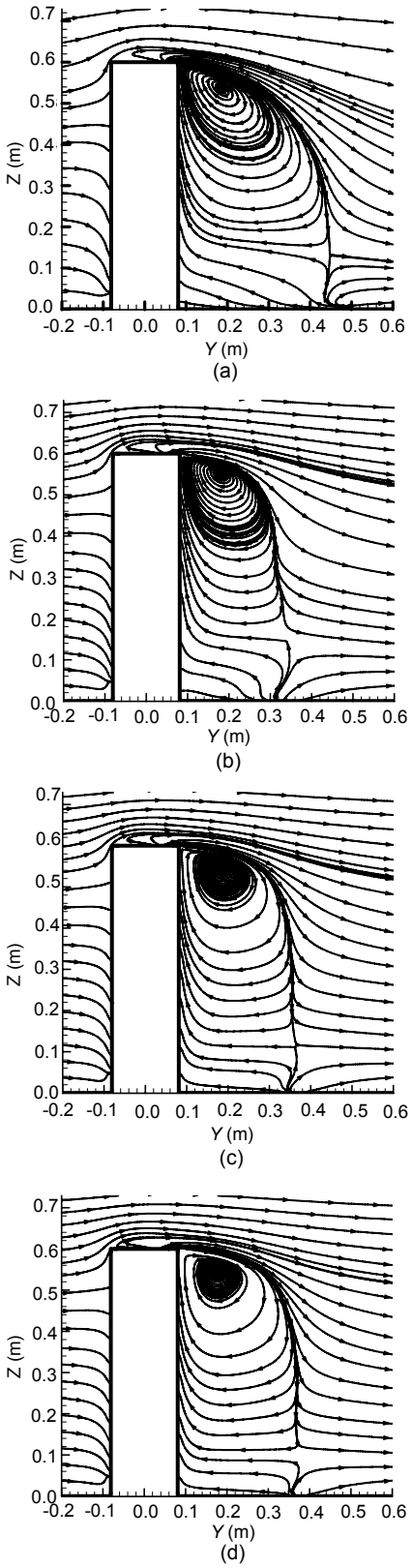

Fig. 13 Comparison of the Reynolds-averaged streamlines around planes x=0 of the models with and without suction
(a) C_Q=0; (b) C_Q=−0.0229; (c) C_Q=−0.0457; (d) C_Q=−0.0686

According to Eqs. (7)–(10), P, C_D' and M_x' are greatly influenced by the orifice geometrical parameters (such as θ and d) and the suction velocities (such as V_c and V_{ca}), and the optimal suction model cannot be put forward directly, but are restricted to the harmony of the relationship among the wind loads of the baseline model, the power input and the equivalent against-wind force.

Furthermore, the overall drag coefficient will be acquired by superposing C_{DC} (the wind-induced drag coefficient for the suction model) and C_D'. When C_{DC} is equal to C_D', the overall drag coefficient for the suction model is equal to zero, and then we call the model a "zero-drag" model. Fig. 14 shows comparisons of C_{DC} and C_D' of the suction models with d=5 mm. For less negative C_Q (C_Q=−0.0229), C_{DC} is much larger than C_D', so the direction of the overall drag coefficient is identical to the wind direction. While for more negative C_Q, the suction models become the "zero-drag" model when θ is close to 30° under C_Q=−0.0457 or located at (45°, 60°) under C_Q=−0.0686.

Using $C_{DR}'=C_D'/C_{DB}$ to denote the quantity of DR contributed by the counterforce induced by suction, and comparisons of C_{DR} and C_{DR}' for the suction models with d=5 mm are shown in Fig. 15. For the suction models with less negative C_Q (such as C_Q=−0.0229) and larger θ, C_{DR} is larger than C_{DR}', so the DR induced by the aerodynamic control is dominating. With increasing increments of the absolute value of C_Q, C_{DR}' is gradually more significant than C_{DR} for the suction models with less θ. Moreover, the overall drag reduction (superposed by C_{DR} and C_{DR}') is very significant. For example, when a suction model has θ=45° and d=5 mm under C_Q=−0.0457 (the power input for suction is P=58.8 W), its overall drag reduction reach to 0.673, so the drag is greatly reduced.

6 Conclusions

After validation of the numerical methods, the DR property for a high-rise building controlled by all-height suction is investigated through the turbulence model of RSM, and the main influence parameters on the performance of drag reduction are analyzed. The main conclusions are summarized as follows.

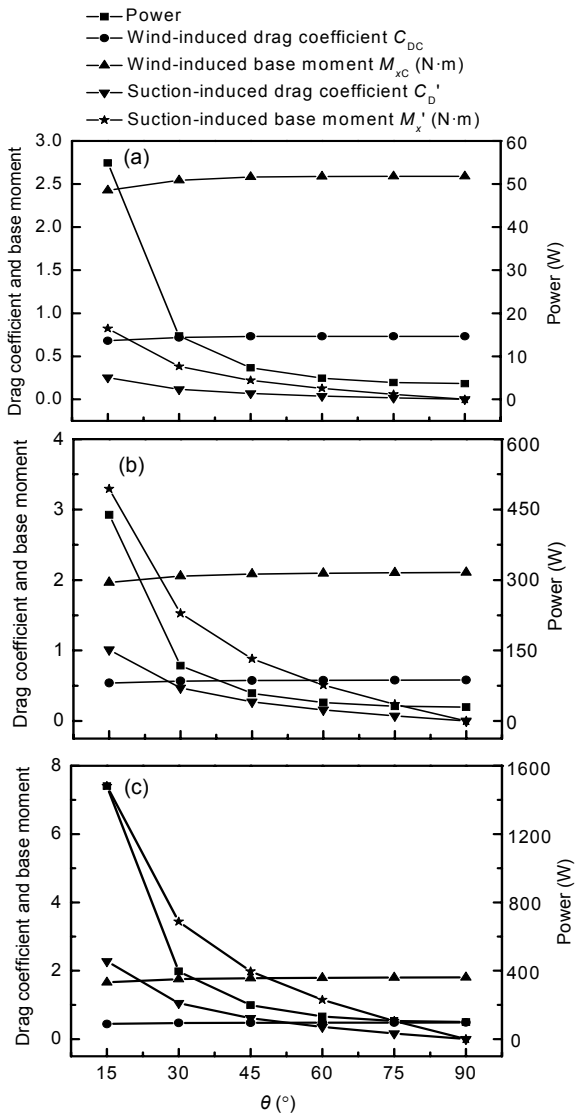

Fig. 14 Wind-induced drag coefficient and base moment, equivalent drag coefficient and base moment for the suction models

(a) C_Q=−0.0229; (b) C_Q=−0.0457; (c) C_Q=−0.0686

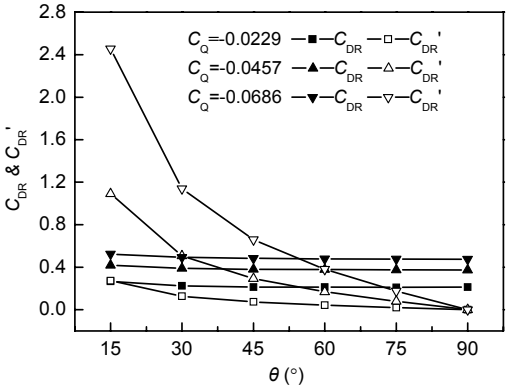

Fig. 15 C_{DR} and C'_{DR} for the suction models

The suction method is very effective on the DR for the high-rise building model, and the sole parameter to determine the DR is the dimensionless suction flux C_Q. With increasing increments of the absolute value of C_Q, the values of C_{PR} for the surfaces, along-wind C_{DR} and C_{MR} of the suction model increase rapidly. Though the orifice geometrical parameters (such as θ and d) and the suction velocities (such as V_c and V_{ca}) show little influence on the DR under the same C_Q, they are strongly related to the energy consumed and the counterforce induced by suction. The detailed flow fields (including the Reynolds-averaged stream and vorticity fields) around the models with and without suction are presented to discuss the mechanism of suction control. It is concluded that suction can bring more flow around the windward face, restrain the flow separation and decrease the curvature of the recirculation and width of the wake.

According to Cheng *et al*. (1996) and Simiu and Scanlan (1996), the Reynolds number effects would have little influence on the flow field and the mean pressure coefficient of the sharp-edged high-rise buildings if the Reynolds number was larger than 1×10^4. Therefore, the results acquired in this paper would have a high applicability for real high-rise buildings (H=180 m) with a high Reynolds number (1×10^7–1×10^8). However, the proposed suction method may yet be some distance from practical application, and some details (mainly on the energy requirement, discomfort for the environment, installation of the suction equipments, and the suction-induced noise) should be further discussed and better-established.

References

Cheng, Z., Shi, Z.C., Zhang, F., 1996. Reynolds number effects in tall building wind tunnel tests. *Journal of Hydrodynamics, Series B*, **4**:56-62.

Fox, R.W., McDonald, A.T., Pritchard, P.J., 2008. Introduction to Fluid Mechanics. John Wiley & Sons Inc., NJ, USA, p.409-446.

GB50009-2001, 2002. Chinese Load Code for Design of Building Structures. Architectural Industry Press of China, Beijing.

Greenblatt, D., Wygnanski, I.J., 2000. The control of flow separation by periodic excitation. *Progress in Aerospace Sciences*, **36**(7):487-545. [doi:10.1016/S0376-0421(00)00008-7]

Huang, L., Huang, P.G., LeBeau, R.P., Hauser, T., 2004.

Numerical study of blowing and suction control mechanism on NACA0012 airfoil. *Journal of Aircraft*, **41**(5):1005-1013. [doi:10.2514/1.2255]

Huang, L., Huang, G., LeBeau, R., Hauser, T., 2007. Optimization of airfoil flow control using a genetic algorithm with diversity control. *Journal of Aircraft*, **44**(4):1337-1349. [doi:10.2514/1.27020]

Kareem, A., Kijewski, T., Tamura, Y., 1999. Mitigation of motions of tall buildings with specific examples of recent applications. *Wind and Structures*, **2**(3):201-251.

Kijewski-Correa, T., Kilpatrick, J., Kareem, A., Kwon, D.K., Bashor, R., Kochly, M., Young, B.S., Abdelrazaq, A., Galsworthy, J., Isyumov, N., *et al.*, 2006. Validating wind-induced response of tall buildings: Synopsis of the Chicago full-scale monitoring program. *Journal of Structural Engineering*, **132**(10):1509-1523. [doi:10.1061/(ASCE)0733-9445(2006)132:10(1509)]

Luo, J.J., Han, D.J., 2009. 3D wind-induced response analysis of a cable-membrane structure. *Journal of Zhejiang University-SCIENCE A*, **10**(3):337-344. [doi:10.1631/jzus.A0820430]

Schlichting, H., Gersten, K., 2000. Boundary-layer Theory (8th Ed.). Mayes, K., Translator. McGraw-Hill, New York, USA, p.291-320.

Simiu, E., Scanlan, R.H., 1996. Wind Effects on Structures: Fundamentals and Applications to Design (3rd Ed.). A Wiley-InterScience Publication, New York, USA, p.144-145, 297-298.

Song, Y.P., Chen, F., Yang, J., Wang, Z.Q., 2005. A numerical Investigation of Boundary Layer Suction in Compound Lean Compressor Cascades. ASME Turbo Expo: Power for Land, Sea, and Air, Reno, USA, p.167-175.

Tu, J.Y., Yeoh, G.H., Liu, C.Q., 2008. Computational Fluid Dynamics: A Practical Approach. Butterworth-Heinemann, Burlington, USA, p.250-271.

Uruba, V., Jonáš, P., Mazur, O., 2007. Control of a channel-flow behind a backward-facing step by suction/blowing. *International Journal of Heat and Fluid Flow*, **28**(4):665-672. [doi:10.1016/j.ijheatfluidflow.2007.04.002]

Zhang, Y.C., Qin, Y., Wang, C.G., 2004. Research on the influence of openings to static wind load of high-rise buildings. *Journal of Building Structures*, **25**(4):112-118 (in Chinese).

Zheng, C.R., 2010. Numerical Investigation of Wind Loads on High-rise Buildings Controlled by Suction/Blowing. PhD Thesis, Harbin Institute of Technology, Harbin, China, p.72-74 (in Chinese).

Zheng, C.R., Zhang, Y.C., 2008. Numerical simulation of mean interference effects for the interfering buildings with different heights. *Journal of Harbin Institute of Technology (New Series)*, **15**(4):499-505.

2009 JCR of Thomson Reuters for *JZUS-A* and *JZUS-B*

ISI Web of Knowledge℠

Journal Citation Reports®

WELCOME | HELP | RETURN TO LIST | PREVIOUS JOURNAL | NEXT JOURNAL

2009 JCR Science Edition

Journal: Journal of Zhejiang University-SCIENCE A

Mark	Journal Title	ISSN	Total Cites	Impact Factor	5-Year Impact Factor	Immediacy Index	Citable Items	Cited Half-life	Citing Half-life
☐	J ZHEJIANG UNIV-SC A	1673-565X	322	0.301		0.066	213	3.0	6.8

Journal: Journal of Zhejiang University-SCIENCE B

Mark	Journal Title	ISSN	Total Cites	Impact Factor	5-Year Impact Factor	Immediacy Index	Citable Items	Cited Half-life	Citing Half-life
☐	J ZHEJIANG UNIV-SC B	1673-1581	619	1.041		0.156	128	3.1	7.5